SCIENTIFIC REPORTS

OPEN

SUBJECT AREAS:
MATERIALS SCIENCE
NANOPARTICLES
QUANTUM CHEMISTRY
MATERIALS CHEMISTRY

Received
28 June 2012

Accepted
6 September 2012

Published
22 October 2012

Correspondence and requests for materials should be addressed to Y.X. (yxie@ustc.edu.cn)

Quantum Tunneling of Magnetization in Ultrasmall Half-Metallic V_3O_4 Quantum Dots: Displaying Quantum Superparamagnetic State

Chong Xiao[1], Jiajia Zhang[1], Jie Xu[1], Wei Tong[2], Boxiao Cao[1], Kun Li[1], Bicai Pan[1], Haibin Su[3] & Yi Xie[1]

[1]Hefei National Laboratory for Physical Sciences at the Microscale, University of Science & Technology of China, Hefei, Anhui, 230026, P.R. China, [2]High Magnetic Field Laboratory, Chinese Academy of Sciences, Hefei, Anhui, 230031, P.R. China, [3]Division of Materials Science, Nanyang Technological University, 50 Nanyang Avenue, 639798, Singapore.

Quantum tunneling of magnetization (QTMs), stemming from their importance for understanding materials with unconventional properties, has continued to attract widespread theoretical and experimental attention. However, the observation of QTMs in the most promising candidates of molecular magnets and few iron-based compounds is limited to very low temperature. Herein, we first highlight a simple system, ultrasmall half-metallic V_3O_4 quantum dots, as a promising candidate for the investigation of QTMs at high temperature. The quantum superparamagnetic state (QSP) as a high temperature signature of QTMs is observed at 16 K, which is beyond absolute zero temperature and much higher than that of conventional iron-based compounds due to the stronger spin-orbital coupling of V^{3+} ions bringing high anisotropy energy. It is undoubtedly that this ultrasmall quantum dots, V_3O_4, offers not only a promising candidate for theoretical understanding of QTMs but also a very exciting possibility for computers using mesoscopic magnets.

For thousands of years, magnetic phenomena as certainly one of the fundamental properties of matter have exercised a remarkable grip on human imagination. One of the most interesting aspects of magnetic materials in modern times is that the observation of unusual properties derived from macroscopic quantum tunneling of magnetization (QTMs)[1]. Due to Heisenberg's uncertainty relation, the quantum mechanical counterparts can show fundamentally different behavior: the present quantum fluctuations may be strong enough to drive a transition from one phase to another, bringing about a macroscopic property change[2–4]. Because of the stem from their importance for understanding materials with unconventional properties, the QTMs has continued to attract widespread theoretical and experimental attention[5,6]. However, observation of the quantum behavior of a macroscopic variable has remained a challenging problem: the extensively presented interest in QTMs of magnetic materials has stemmed largely from studies of molecular magnets[7–9], which is difficult in development because of the problem in the design of prerequisite genuine three-dimensional connected lattices in molecular magnets[10].

In contrast to molecular magnets with very complex structures, artificial nanoscale systems could offer a new and simple means of observing and understanding QTMs[11]. Taking ferromagnetic compound as example, one of the most interesting aspects of the behavior of a ferromagnetic material is the fact that the superparamagnetic (SP) appears when its size decreases to a critical value. Such behavior may have important consequences in determining the lifetime of magnetic information storage when using nanoscale magnets[12,13]. While the classically thermal-assisted SP should be blocked because the thermal fluctuation of the random spin orientation is frozen and causing a long-range magnetic order as temperature decreases. That is to say, the SP disappear when the thermal energy cannot overcome the magnetic energy barrier. If the size further reduces to small enough, the QTMs take place as temperature further decreases: dramatic increase in surface to volume ratio causes strong surface anisotropic field, which provides channels for quantum tunneling between spin-glass and quantum paramagnet, thus one can re-observe the SP state even when the thermal energy is smaller than the barrier height and denote as QSP[14,15] offers a very exciting possibility for computers using mesoscopic magnets for memory[16]. Magnetic quantum tunneling in quantum dots is of fundamental importance, not only for potential information

Table 1 | Summary of the blocking (T_B) and crossover temperature (T_C) for some nanomaterials

Materials	Average Size (nm)	T_B (K)	T_C (K)	Ref.
γ-Fe_2O_3	5	220	2.2	17
FeC	3.6	20	1	18
$CoFe_2O_4$ (in water)	3	170	2.5	19
$CoFe_2O_4$ (in silicate)	3	170	5	19
FeOOH	3	47	7	20
$NiFe_2O_4$	7	170	2	21
ferritin	8	13	2.1	22

and computation application but also because it presents possibility to deal experimentally with a single quantum object of mesoscopic size. Moreover, owing to the nanometric confinement of the electrons, quantum dots display relatively high energy scales that allow the observation of interesting QTMs phenomena at accessible temperatures, rather than absolute zero temperature[11]. Many recent observation of QTMs in iron-based compounds nanoparticles have shown that the crossover temperature beyond absolute zero temperature, which indicate that the QTMs does not necessarily have to be in the vicinity of absolute zero temperature (seen in **Table 1**). However, it is still high temperature limited. Thus, it is necessarily to search new and simple system for understanding the difference between theoretical predictions and experimental observation, e.g. the QTMs does not take place at absolute zero temperature, and if can we obtain materials with even higher crossover temperature of QTMs.

Vanadium oxides, as typical transition metal oxides, have attracted extensive attention for their unique electrical properties due to the prolific valence state of vanadium ion[23]. It is interesting that almost all of the binary vanadium oxides can be expressed as a simple formula: V_nO_{2n-1} (n is a integer $\geq$ 1) or V_nO_{2n+1} (n is a integer $\geq$ 2)[24], while, it is exception for V_3O_4, because of the lack of an identified integer to conform above simple formula. In fact, V_3O_4 crystallized in cubic lattice with constants a=8.457 Å is an isomorphism of Fe_3O_4 (**Figure 1a**), which has inverse spinel structure of AB_2O_4[25]. In this structure, the octahedral six-coordinated B sites, twice as abundant as the A sites, are equally occupied by V^{3+} and V^{2+}, whereas the tetrahedral four-coordinated A sites are occupied by the remaining V^{3+}. The most prominent and interest feature of this structure is the presence of a half-metallic state due to the spin state of different site vanadium ions. The first-principles density functional theory (DFT) calculation results indicate that V_3O_4 is also of half-metallic feature: the calculated density of states (DOS) curves of the spin-down states show a broad band gap, whereas the curves of the spin-up states exhibit gapless which are actually originated from the 3d states of V^{3+} and V^{2+} locating at B sites (**Figure 1b, c**). This half-metallic state due to the spin-up and spin-down levels of vanadium ions existing at the Fermi level may leads to efficient ferromagnetic *p-d* exchange, thus, one may expect to observe the potential QTMs from long-range order ferromagnetism to QSP[26,27]. On the other hand, due to the different strength of spin-orbital coupling in vanadium ions compared to the other conventionally considered transition metal ions (*e.g.* iron, cobalt or nickel, of which most possess more than five *d* electrons), it is reasonably expected that the V_3O_4 quantum dots should behave different magnetic properties compared to those conventional iron-based spinel compounds, such as crossover temperature of QTMs.

Herein, we first put forward the half-metallic V_3O_4 quantum dots as a promising and simple candidate for the investigation of QTMs. The ultramall V_3O_4 quantum dots with average size of 4.8 nm was first successfully synthesized through a simple solvothermal method. As expected, due to the ferromagnetic *p-d* exchange deriving from the spin-up and spin-down states of different sites' vanadium ions, the superparamagnetic state was observed when the size of ferromagnetic bulk reduce to below critical size at room temperature. The clear-cut evidences in temperature dependent magnetization, magnetic relaxation and EPR confirmed that the SP state was blocked as the temperature decreases to 32 K, while was re-observed below 16 K due to the quantum tunneling. This quantum criticality temperature of QTMs, 16 K, is much higher than that of Fe based compounds. More importantly, it is undoubtedly that the new ultrasmall quantum dots, V_3O_4, offer not only a promising candidate for theoretical understanding of QTMs but also a very exciting possibility for computers using mesoscopic magnets for memory.

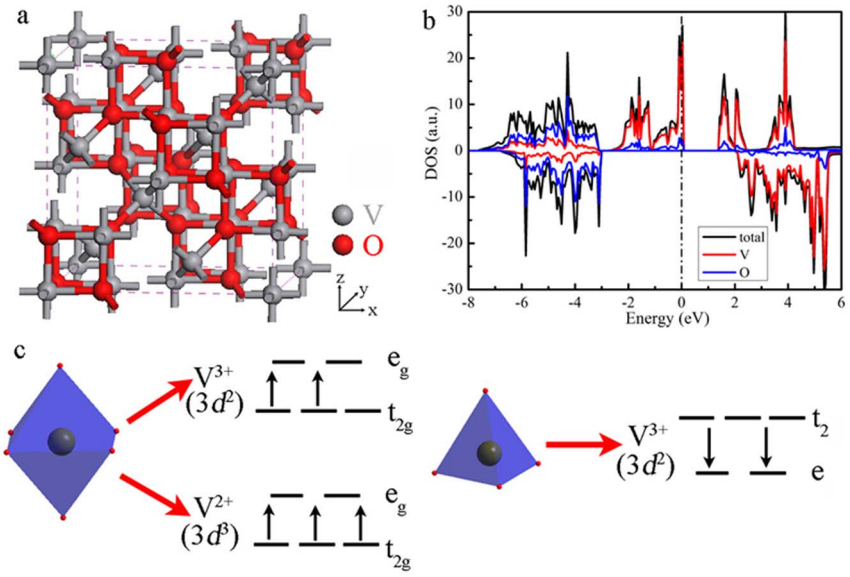

Figure 1 | Schematic representation of the crystal and electronic structure for V_3O_4. (a) Unit cell of V_3O_4; (b) The calculated DOSs of the V_3O_4. The DOSs above zero are corresponding to the spin-up states, and the other to the spin-down states; (c) Schematic spin structure of V^{3+} and V^{2+} in octahedral and tetrahedron sites, respectively.

Results

Inspired by the above structural and electronic band structure analysis, we synthesized ultrasmall V_3O_4 quantum dots through a simple solvothermal method for the first time. The phase purity and crystal structure of the as-prepared products were examined by XRD and the results are shown in **Figure 2a**. The XRD pattern of V_3O_4 quantum dots match well with the standard cubic V_3O_4 (space group: Fd-3m) with lattice constants a=8.457 Å, (JCPDS 34-0615). Slight peak broadening of the XRD peaks of V_3O_4 nanoparticles was primarily due to the small size of V_3O_4 nanoparticles. The direct information for the valence state of the as-prepared products can be provided by the analysis of the surface molecular and electronic structure of the products by XPS, which are shown in **Figure 2b**. The binding energies of O_{1S} at 530.3 eV can be assigned to the O^{2-} [28]. The high-resolution XPS for the V_{2p} region shows that there are two contributions here: the core level at 523.0 eV and 515.3 eV are attributed to the spin-orbit splitting of the components, $V_{2p3/2}$ and $V_{2p1/2}$, which is in agreement with the literature values for V^{3+}, while the core level at 521.4 eV and 514.1 eV with the minor V signal assigned to V^{2+} [29]. Taking into account the atomic sensitivity factors of V and O, the atomic ratio of V/O is approximately 3 : 4 according to quantification of the peak areas of V 2p and O 1s. No peaks of other impurity and elements are observed in XRD pattern and XPS survey spectrum, indicating the high purity of the as-prepared V_3O_4 quantum dots. The size and shape of as-obtained V_3O_4 quantum dots was examined by TEM and HRTEM. As shown in **Figure 2c**, we can see the V_3O_4 quantum dots sized in an average diameter of 4.8 nm with nearly spherical shapes. The TEM images also display the particle size distributions (see the insert of **Figure 2c**). The HRTEM images (**Figure 2d**) of one individual nanocrystal indicated the distances between the adjacent lattice fringes to be 2.52 Å which corresponds with the lattice spacing of the (311) d-spacing for cubic V_3O_4 (2.548 Å, JCPDS 34-0615).

Temperature dependence of zero-field-cooled (ZFC) magnetization, field-cooled (FC) magnetization and magnetic field dependence of magnetization (M-H) curves were carried out to study the magnetic property of the ultrasmall V_3O_4 quantum dots, which were measured with a superconducting quantum interference device (SQUID) magnetometer. **Figure 3a** shows the variation of the magnetization as a function of temperature under field-cooled (FC) and zero-field-cooled (ZFC) conditions with applied magnetic fields of 200 Oe. The observed blocking temperature (T_B) deduced from ZFC measurements is 32 K. More interesting, another transition at lower temperature was also observed: ZFC magnetization decreases as the temperature rises from 4 K, reaches a minimum near temperature T_C of 16 K, and starts increasing from this point to the blocking temperature T_B at 32 K. This remarkable transition point gives a clear-cut evidence of QTMs from magnetic long-range order to QSP state in V_3O_4 quantum dots at 16 K. Further evidence of the crossover temperature of QTMs at 16 K producing the anomalous magnetization behavior can be observed by inspection of the reciprocal susceptibility χ^{-1} for V_3O_4 quantum dots (insert of **Figure 3a**). The linear curve characterized with 1/T dependence in reciprocal susceptibility χ^{-1} as a reflection also clearly shows the QSP behavior of V_3O_4 quantum dots below 16 K. It is worth to underlining that this quantum critical temperature at 16 K with QSP state as a high temperature signature of QTMs is much higher than that of conventional iron-based compounds, which should derive from the strong L-S coupling of octahedral sites' V^{3+} ions in V_3O_4. **Figure 3b** shows the magnetic-field dependence of magnetization (M *vs* H) at 300 K and 4 K for as-prepared V_3O_4 quantum dots after subtracting the paramagnetic background from the raw data. At room temperature, the negligible remnant magnetization and coercivity in hysteresis loops indicate that the V_3O_4 quantum dots behave as SP.

As well known, the magnetic behavior of a small particle depends on its relaxation time. In a real system of small particles, when a magnetic field, orienting the moments of identical particles, is removed, the time dependence of the magnetic moment of the system is governed by the logarithmic law[19]:

$$M(t) = M(t_0)[1 - S\ln(t/t_0)] \quad (1)$$

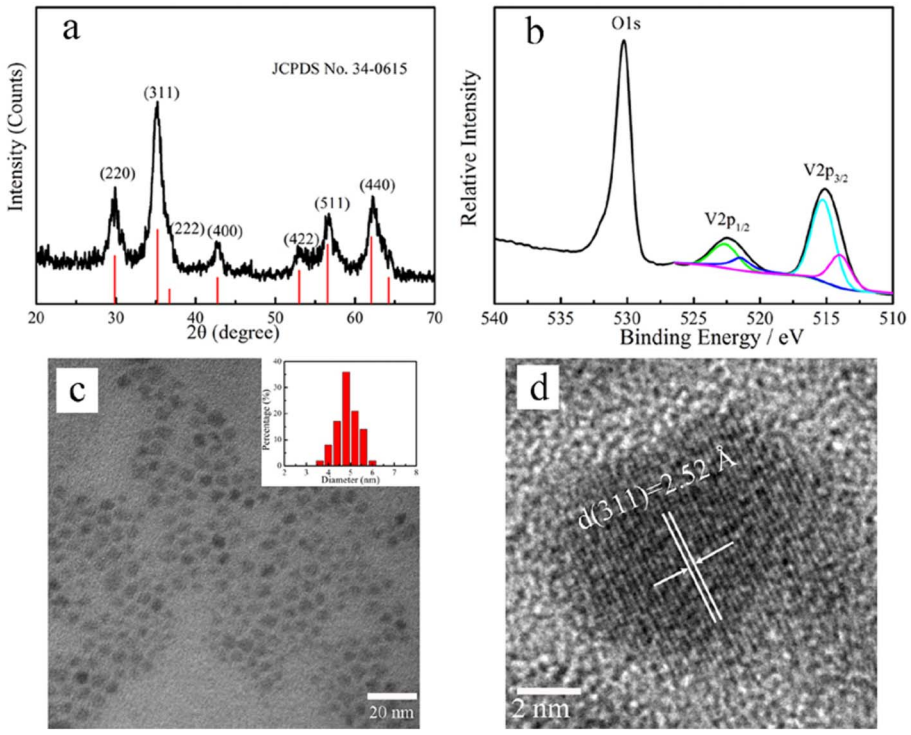

Figure 2 | Characterization of as-obtained ultrasmall V_3O_4 quantum dots. (a) XRD pattern, (b) XPS spectrum, (c) TEM image, and (d) HRTEM image for as-prepared V_3O_4 quantum dots.

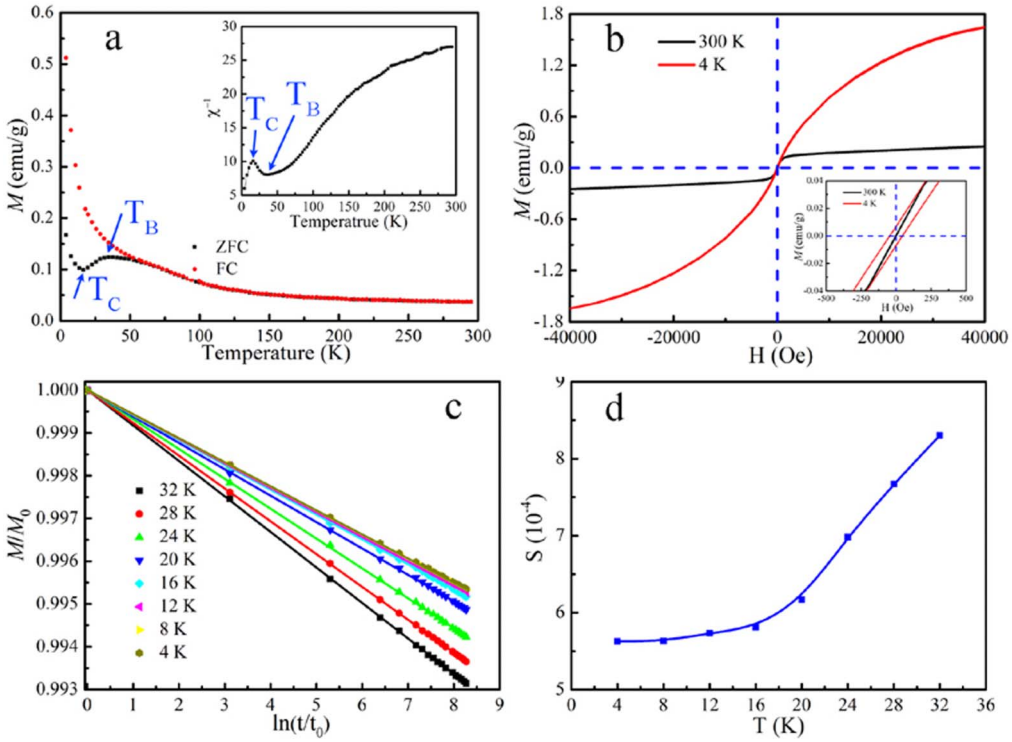

Figure 3 | Magnetic properties for as-obtained V_3O_4 quantum dots. (a) Magnetization versus temperature for field cooled (FC) and zero-field-cooled (ZFC) measurements. The blocking temperature (T_B) and the critical phase transition temperature (T_C) are indicated on the ZFC data set. Inset represent the variation in inverse magnetization with temperature; (b) Magnetization as a function of field for V_3O_4 quantum dots at 300 and 4 K and inset of the hysteresis behavior; (c) Magnetization vs logarithm of time obtained in the relaxation measurements; (d) Magnetic viscosity extracted from the relaxation data as a function of temperature for the V_3O_4 quantum dots.

$$S(T) = \frac{k_B T}{\langle U \rangle} \tag{2}$$

here $S(T)$ is the magnetic viscosity, t_0 is an arbitrary time after changing the field, $\langle U \rangle$ is the average energy barrier, k_B the Boltzmann constant and T is the absolute temperature. At the thermally activated regime, $T_C < T < T_B$, S is proportional to T, and at the quantum-tunneling-dominated regime $T < T_C$, S=const. Thus, a fundamental understanding to the dynamic behavior of the magnetization vector of small particles during the QTMs can be obtained through the magnetic relaxation measurement. In this study, the magnetic relaxation experiments were performed in following procedures: first the V_3O_4 quantum dots sample was cooled in an applied field $H_1 = 200$ Oe to a target temperature, after which the applied field was changed to $H_2 = -200$ Oe, then the change of remnant magnetization with time was measured for a few hours. After this measurement, the sample was cooled to lower temperature with applied field H_1 and then the applied field was changed to H_2 for other relaxation measurements. In **Figure 3c**, we plot the magnetization versus logarithmic time ($M(t)/M(t_0) \sim \ln(t/t_0)$, with $t_0 = 1$s) obtained in the relaxation measurements, at different sample temperatures. The best fitting to the time dependence of the magnetization is the logarithmic time law (Eq. (1)). The magnetic viscosity $S(T)$ can be extracted from the relaxation data. As shown in **Figure 3d**, it is clear that between 32 and 16 K, the viscosity changes linearly with temperature, which corresponds to the thermally activated relaxation of the magnetization. While the viscosity begins to be temperature independent at temperature below 16 K, which is the signature of quantum tunneling of magnetization and in agreement with the result of ZFC measurement.

Further insight into the QTMs requires investigation of the electron spin resonance (ESR) measurement for the quantum dots sample. The temperature-dependent ESR spectra of V_3O_4 quantum dots from 6 to 300 K are specified by curves as shown in **Figure 4**. Although the dominant resonance positions for the ESR do not shift probably as the temperature decrease from 300 to 6 K, a clear variation of the ESR occurs in low field at the temperature below 40 K. A broad resonance feature at low field, which usually is a signal of ferromagnetism, appears at 32 K and disappears at 16 K, which is consistent with the results of ZFC and magnetic relaxation experiments: as temperature decreases, the QTMs causing transition from long-range order to QSP at 16 K in V_3O_4 quantum dots. The temperature-dependent peak-to-peak linewidth (shown in **Figure 4c**) also clearly reflects the QTMs. The anomalous linewidth broadening below 16 K is indicative of a magnetic phase transition within the sample and has been interpreted as a QTMs behavior for ferrous oxides at the nanoscale[27,30]. In fact, the presence of a half-metallic state due to the spin-up and spin-down levels of vanadium ions existing at the Fermi level (see in **Figure 1**) should lead to efficient ferromagnetic *p-d* exchange. At high temperature ($T > 32$ K), the thermal activation energy can overcome the barrier, and thus the nanoparticles behave as a single magnetic domain, exhibiting SP behavior, whereas at temperature below the blocking temperature 32 K, the p-d exchange becomes stronger and results in the ferromagnetism. As the temperature further decreases to below 16 K, the strong surface anisotropic field provides the quantum tunneling and results in the QTMs from ferromagnetism to QSP.

Discussions

As described in the above experimental results, clear-cut evidences in temperature-dependent magnetization, magnetic relaxation and EPR all confirmed that the SP state was blocked as the temperature decreases to 32 K, while was re-observed below 16 K due to the QTMs. It is worth noting that the QTMs temperature of V_3O_4

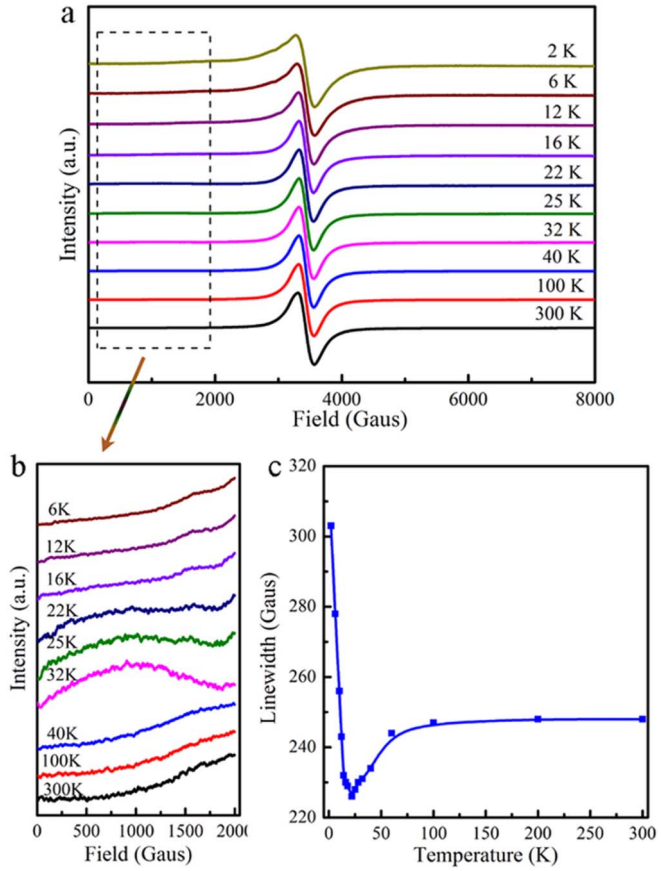

Figure 4 | Temperature-dependent ESR for V_3O_4 quantum dots. (a) The temperature-dependent ESR spectra for V_3O_4 measured at various temperatures from 4 to 300 K; (b) Magnified ESR spectra at field range of 0 to 2000 Gauss for V_3O_4 quantum dots; (c) Plot of linewidth of the ESR spectra as a function of temperature.

quantum dots is much higher than those of conventional iron-based spinel compounds. It is well known that the temperature of QTMs from blocked SP state to QSP state is proportional to the anisotropy energy of nanoparticles[15], which is determined by the strength of spin-orbital coupling according to the Stoner-Wohlfarth theory for single-domain nanoparticle[31]. In this study, It is found that the *d* electrons of vanadium ions display the configurations $t_{2g}^2e_g^0$, $t_{2g}^3e_g^0$ and $e^2t_2^0$ at the octahedral, octahedral and tetrahedral lattice sites for V^{3+}, V^{2+} and V^{3+} ions, respectively (see in **Figure 1c**). As a result, the coupling between the electron spin and the angular momentum of its orbital (L-S coupling) should only derive from the octahedral sites' V^{3+} ions with a multiplet ground state of $^3T_{1g}$. While for others iron based spinel compounds, the Fe^{3+} ions occupy the octahedral sites with $^6A_{1g}$, and the others transition metals occupy tetrahedral lattice sites, which usually result in ground state A or E, such as ^5E for Fe^{2+} and $^4A_2$ for Co^{2+}. Because the angular momentum is quenched in these ground states of A and E, V_3O_4 should exhibit stronger L-S coupling compared to that of the other transition metal iron based spinel compounds, which may result larger anisotropy energy. Thus, higher QTMs temperature of V_3O_4 quantum dots compared to those iron based compounds was observed in this study.

In summary, ultrasmall V_3O_4 quantum dots were successfully synthesized through a facile solvothermal method, and its magnetic property was systematically investigated for the first time. The QSP state as a high temperature signature of QTMs is firstly observed in V_3O_4 quantum dots, which is much higher than that of conventional iron-based compounds. We conclude that the spin-orbital coupling resulting in the high anisotropy energy should contribute to the high crossover temperature of QTMs, which established the direct correlation between spin-orbital coupling with the temperature of quantum tunneling of magnetization. This intriguing observation enables the ultrasmall half-metallic V_3O_4 quantum dots not only a simple promising candidate for the investigation of QTMs but also a very exciting possibility for computers using mesoscopic magnets for memory.

Methods

Synthesis of V_3O_4 quantum dots. All chemicals were of analytic grade purity obtained from Sinopharm Chemical Reagent Co., Ltd and used as received without further purification. V_3O_4 quantum dots were synthesized through a simple solvothermal method. Briefly, 0.6 mmol vanadium acetylacetonate were added into 25 ml oleylamine in a 50.0 mL flask. In order to dissolve the mixture, the suspension solution was heated to 100°C under magnetically stirred. After the mixture was completely dissolved, the black solution was sealed in a 40 ml autoclave and heated at the temperature of 220°C for 20 h. The system was then allowed to cool to room temperature. The final V_3O_4 samples were separated from the resulting solution by centrifuging and washed several times with ethanol and cyclohexane to remove any possible ionic remnants, then dried in a vacuum at 60°C.

Characterization. The structure of these obtained samples was characterized with the X-ray diffraction (XRD) pattern, which was recorded on a Rigaku Dmax diffraction system using a Cu Kα source (λ=1.54187 Å). X-ray photoelectron spectroscopy (XPS) measurements were performed on a VGESCALAB MK II X-ray photoelectron spectrometer with an excitation source of Mg Kα=1253.6 eV. High-resolution transmission electron microscopy (HRTEM) images were performed on JEOL-2010 transmission electron microscope at 200 kV. The magnetic measurement was carried out with a superconducting quantum interference device magnetometer (Quantum Design MPMS XL-7). The temperature-dependent EPR measurement of the powder sample was performed using a Bruker EMX plus model spectrometer operating at X-band frequencies (9.4 GHz) at different temperatures.

Calculations. All calculations were performed using density functional theory as implemented in the Vienna ab initio simulation program (VASP)[32]. The LSDA plus on-site Coulomb interaction U scheme was adopted to treat the electron-electron correlation[33]. The plane-wave cut-off energy was set to 550 eV. We had tested different U values, but all calculations resulted in the same half-metal ferromagnetic ground state for V_3O_4. Here we reported only the results of U=4.5 eV.

1. Chudnovsky, E. M. & Tejada, T. Quantum Tunneling of the Magnetic Moment, Cambridge University Press, 1998.
2. Greiner, M., Mandel, O., Esslinger, T., Hänsch, T. W. & Bloch, I. Quantum phase transition from a superfluid to a Mott insulator in a gas of ultracold atoms. *Nature* **415**, 39–44 (2002).
3. Si, Q. M. & Steglich, F. Heavy Fermions and Quantum Phase Transitions. *Science* **329**, 1161–1166 (2010).
4. Si, Q. M., Rabello, S., Ingersent, K. & Smith, J. L. Locally critical quantum phase transitions in strongly correlated metals. *Nature* **413**, 804–808 (2001).
5. Rønnow, H. M. *et al.* Quantum Phase Transition of a Magnet in a Spin Bath. *Science* **308**, 389–392 (2005).
6. Knafo, W., Raymond, S., Lejay, P. & Flouquet, J. Antiferromagnetic criticality at a heavy-fermion quantum phase transition. *Nat. Phys.* **5**, 753–757 (2009).
7. Mannini, M. *et al.* Quantum tunnelling of the magnetization in a monolayer of oriented single-molecule magnets. *Nature* **468**, 417–421 (2010).
8. Burzurí, E. *et al.* Magnetic Dipolar Ordering and Quantum Phase Transition in an Fe_8 Molecular Magnet. *Phys. Rev. Lett.* **107**, 097203 (2011).
9. Das, A. *et al.* A New Family of 1D Exchange Biased Heterometal Single-Molecule Magnets: Observation of Pronounced Quantum Tunneling Steps in the Hysteresis Loops of Quasi-Linear $\{Mn_2Ni_3\}$ Clusters. *J. Am. Chem. Soc.* **133**, 3433–3443 (2011).
10. Gatteschi, D. & Sessoli, R. Quantum Tunneling of Magnetization and Related Phenomena in Molecular Materials. *Angew. Chem. Int. Ed.* **42**, 268–297 (2003).
11. Roch, N., Florens, S., Bouchiat, V., Wernsdorfer, W. & Balestro, F. Quantum phase transition in a single-molecule quantum dot. *Nature* **453**, 633–638 (2008).
12. Deng, Y., Qi, D., Deng, C., Zhang, X. & Zhao, D. Superparamagnetic High-Magnetization Microspheres with an Fe3O4@SiO2 Core and Perpendicularly Aligned Mesoporous SiO_2 Shell for Removal of Microcystins *J. Am. Chem. Soc.* **130**, 28–29 (2008).
13. Bao, N. Z. *et al.* Controlled Growth of Monodisperse Self-Supported Superparamagnetic Nanostructures of Spherical and Rod-Like $CoFe_2O_4$ Nanocrystals. *J. Am. Chem. Soc.* **131**, 12900–12901 (2009).
14. Hsieh, C. T. & Lue, J. T. Anisotropy-induced quantum critical behavior of magnetite nanoparticles at low temperatures. *Phys. Lett. A* **300**, 636–640 (2002).
15. Hsieh, C. T. & Lue, J. T. Anisotropy-induced quantum superparamagnet state in cobalt-ferrite nanoparticles at low temperatures. *Phys. Lett. A* **316**, 329–335 (2003).
16. Tejada, J., Ziolo, R. F. & Zhang, X. X. Quantum Tunneling of Magnetization in Nanostructured Materials. *Chem. Mater.* **8**, 1784–1792 (1996).

17. Zhang, X. X., Ziolo, R. F., Kroll, E. C., Bohigas, X. & Tejada, J. Magnetic relaxation and quantum tunneling in nanocrystalline particles. *J. Magn. Magn. Mater.* **140–144**, 1853–1854 (1995).
18. Balcells, L. L. *et al*. Quantum tunneling of magnetization in metallic FeC ferrofluids. *Z. Phys. B: Condens. Matter.* **89**, 209–212 (1992).
19. Zhang, X. X., Hernandez, J. M., Tejada, J. & Ziolo, R. F. Magnetic properties, relaxation, and quantum tunneling in $CoFe_2O_4$ nanoparticles embedded in potassium silicate. *Phys. Rev. B* **54**, 4101–4106 (1996).
20. Ibrahim, M. M., Darwish, S. & Seehra, M. M. Nonlinear temperature variation of magnetic viscosity in nanoscale FeOOH particles. *Phys. Rev. B* **51**, 2955–2959 (1995).
21. Kodama, R. H., Seaman, C. L., Berkowitz, A. E. & Mapple, B. Low-temperature magnetic relaxation of organic coated $NiFe_2O_4$ particles. *J. Appl. Phys.* **75**, 5639–5641 (1994).
22. Tejada, J. & Zhang, X. X. On magnetic relaxation in antiferromagnetic horse-spleen ferritin proteins. *J. Phys.: Condens. Matter.* **6**, 263–266 (1994).
23. Wu, C. Z., Wei, H., Ning, B. & Xie, Y. New Vanadium Oxide Nanostructures Controlled Synthesis and Their Smart Electrical Switching Properties. *Adv. Mater.* **22**, 1972–1976 (2010).
24. Schwingenschlogl, U. & Eyert, V. The vanadium Magneli phases V_nO_{2n-1}. *Ann. Phys. (Leipzig)* 2004, **13**, 475–510.
25. Anan'in, A. V., Breusov, O. N., Dremin, A. N., Drobyshev, V. N. & Pershin, S. V. Physicochemical Transformations of Vanadium Pentoxide Under the Influence of Shock Waves. *Russ. J. Inorg. Chem.* **20**, 319–321 (1975).
26. Zhang, C. W., Yan, S. S., Wang, P. J. & Zhang, Z. Half-metallic ferromagnetism in $Cd_{1-x}TM_xSe$ (TM = Cr, V and Mn) semiconductors. *Comput. Mater. Sci.* **43**, 710–714 (2008).
27. Zheng, W. W. *et al*. Quantum Phase Transition from Superparamagnetic to Quantum Superparamagnetic State in Ultrasmall $Cd_{1-x}Cr(II)_xSe$ Quantum Dots. *J. Am. Chem. Soc.* **134**, 2172–2179 (2012).
28. Xu, Y., Zheng, L., Wu, C. Z., Qi, F. & Xie, Y. New-Phased Metastable V_2O_3 Porous Urchinlike Micronanostructures: Facile Synthesis and Application in Aqueous Lithium Ion Batteries. *Chem. Eur. J.* **17**, 384–391 (2011).
29. Nivoix, V. & Gillot, B. Intermediate valencies of vanadium cations appearing during oxidation of vanadium-iron spinels. *Mater. Chem. Phys.* 2000, **63**, 24–29 (2000).
30. Gider, S., Awschalom, D. D., Douglas, T., Mann, S. & Chaparala, M. Classical and quantum magnetic phenomena in natural and artificial ferritin proteins. *Science* **268**, 77–80 (1995).
31. Liu, C., Zou, B. S., Rondinone, A. J. & Zhang, Z. J. Chemical Control of Superparamagnetic Properties of Magnesium and Cobalt Spinel Ferrite Nanoparticles through Atomic Level Magnetic Couplings. *J. Am. Chem. Soc.* **122**, 6263–6267 (2000).
32. Kresse, G. & Furthmuller, J. Efficient iterative schemes for *ab initio* total-energy calculations using a plane-wave basis set. *Phys. Rev. B* **54**, 11169–11186 (1996).
33. Anisimov, V. I., Zaanen, J. & Andersen, O. K. Band theory and Mott insulators: Hubbard U instead of Stoner I. *Phys. Rev. B* **44**, 943–954 (1991).

Acknowledgements

The authors thank Prof. Jinlong Yang and Zhenyu Zhang in the University of Science & Technology of China for their useful discussions about the magnetic properties.
This work was financially supported by National Basic Research Program of China (No. 2009CB939901), National Natural Science Foundation of China (11079004, 90922016, 10979047), innovation project of Chinese Academy of Science (KJCX2-YW-H2O).

Author contributions

C.X. and Y.X. conceived the idea and co-wrote the paper. C.X., J.X., K.L. and B.X.C. carried out the examples synthesis, characterization. J.J.Z., B.C.P. and H.B.S. carried out the theoretical calculations. Temperature dependent ESR experiments were recorded and interpreted by C.X. and W.T. All the authors discussed the results, commented on and revised the manuscript.

Additional information

Competing financial interests: The authors declare no competing financial interests.

How to cite this article: Xiao, C. *et al*. Quantum Tunneling of Magnetization in Ultrasmall Half-Metallic V_3O_4 Quantum Dots: Displaying Quantum Superparamagnetic State. *Sci. Rep.* **2**, 755; DOI:10.1038/srep00755 (2012).